REPORT DOCUMENTATION PAGE

Form Approved OMB NO. 0704-0188

1. REPORT DATE (DD-MM-YYYY)	2. REPORT TYPE	3. DATES COVERED (From - To)
01-08-2017	Final Report	1-Oct-2016 - 30-Jun-2017

4. TITLE AND SUBTITLE
Final Report: Molecular Beam Epitaxial Growth and Characterization of Two-Dimensional BN/MoxW1-xSe2 Heterostructures

5a. CONTRACT NUMBER
W911NF-16-1-0582

5b. GRANT NUMBER

5c. PROGRAM ELEMENT NUMBER
611102

6. AUTHORS

5d. PROJECT NUMBER

5e. TASK NUMBER

5f. WORK UNIT NUMBER

7. PERFORMING ORGANIZATION NAMES AND ADDRESSES
University of Michigan - Ann Arbor
3003 South State Street

Ann Arbor, MI 48109 -1274

8. PERFORMING ORGANIZATION REPORT NUMBER

9. SPONSORING/MONITORING AGENCY NAME(S) AND ADDRESS (ES)
U.S. Army Research Office
P.O. Box 12211
Research Triangle Park, NC 27709-2211

10. SPONSOR/MONITOR'S ACRONYM(S)
ARO

11. SPONSOR/MONITOR'S REPORT NUMBER(S)
69837-EL-II.1

12. DISTRIBUTION AVAILIBILITY STATEMENT
Approved for public release; distribution is unlimited.

13. SUPPLEMENTARY NOTES
The views, opinions and/or findings contained in this report are those of the author(s) and should not contrued as an official Department of the Army position, policy or decision, unless so designated by other documentation.

14. ABSTRACT

15. SUBJECT TERMS

16. SECURITY CLASSIFICATION OF:			17. LIMITATION OF ABSTRACT	15. NUMBER OF PAGES	19a. NAME OF RESPONSIBLE PERSON
a. REPORT	b. ABSTRACT	c. THIS PAGE			Zetian Mi
UU	UU	UU	UU		19b. TELEPHONE NUMBER 734-764-3963

RPPR Final Report
as of 01-Sep-2017

Agency Code:

Proposal Number: 69837ELII **Agreement Number: W911NF-16-1-0582**
INVESTIGATOR(S):

Name: Zetian Mi
Email: ztmi@umich.edu
Phone Number: 7347643963
Principal: Y

Organization: **University of Michigan - Ann Arbor**
Address: 3003 South State Street, Ann Arbor, MI 481091274
Country: USA
DUNS Number: 073133571 EIN: 386006309
Report Date: 30-Sep-2017 Date Received: 01-Aug-2017
Final Report for Period Beginning 01-Oct-2016 and Ending 30-Jun-2017
Title: Molecular Beam Epitaxial Growth and Characterization of Two-Dimensional BN/MoxW1-xSe2 Heterostructures
Begin Performance Period: 01-Oct-2016 **End Performance Period:** 30-Jun-2017
Report Term: 0-Other
Submitted By: Zetian Mi Email: ztmi@umich.edu
Phone: (734) 764-3963
Distribution Statement: 1-Approved for public release; distribution is unlimited.

STEM Degrees: 0 **STEM Participants:** 0

Major Goals: The transition-metal dichalcogenide (TMDC) semiconductors, including MoS2, WS2, MoSe2, WSe2, MoTe2, and WTe2 are indirect bandgap in their bulk case with a crossover to direct bandgap semiconductors in a monolayer limit due to quantum confinement effects. The exciton oscillator strengths in such layer-structured 2D materials are exceptionally large, due to the very large exciton binding energies (0.5 – 1 eV). Therefore, such emerging 2D materials provide a nearly ideal platform for the exploitation of exciton-polaritons, the mixed states of photon and exciton, to realize room-temperature operational ultralow threshold polariton lasers with phase coherence and intensity stability comparable to that of conventional photon lasers. To date, however, it has remained challenging for the controlled synthesis of 2D TMDC semiconductors and related van der Waals heterostructures with superior quality and clean interfaces. Hexagonal boron nitride (h-BN) is an ideal template for the growth of TMDCs, which can lead to reduced dielectric screening and large exciton binding energy.

In this project, we aim to investigate the synthesis and properties of 2D TMDC and BN using molecular beam epitaxy (MBE), the champion semiconductor growth technology which offers ultimate control down to atomic layer in an ultrahigh vacuum environment. We will study the MBE growth and structural and optical properties of 2D TMDCs including WTe2 and WSe2, as well as h-BN. The capacity to epitaxially grow superior quality monolayer TMDC and h-BN by MBE will provide a viable approach for the monolithic integration of various monolayer 2D heterostructures and nanostructures with access to unprecedented material quality, complexity, and degree of control, which is critical for their emerging device applications, including the realization of high temperature polariton lasers.

Accomplishments: Please see attached pdf file.

Training Opportunities: PhD student David Laleyan has been trained on the MBE growth of 2D TMDC and BN nanostructures.

Results Dissemination: 1. “Effect of growth temperature on the structural and optical properties of hexagonal boron nitride by molecular beam epitaxy”, D. A. Laleyan, S. Zhao, Y. Wang and Z. Mi, Appl. Phys. Lett., in preparation.
2. “Magnetic-field-enhanced superconductivity in epitaxial thin film WTe2”, T. Asaba, Y. Wang, G. Li, B. J. Lawson, C. Tinsman, L. Chen, S. Zhao, D. Laleyan, Z. Mi, L. Li, Phys. Rev. Lett., under review.
3. “Wafer-scale synthesis of monolayer WSe2: A multi-functional photocatalyst for efficient overall pure water splitting”, Y. Wang, S. Zhao, Y. Wang, D. Laleyan, C.-H. Soh, Y. Wu, and Z. Mi, Nano Lett., in preparation.

RPPR Final Report
as of 01-Sep-2017

Honors and Awards: Zetian Mi was elected Fellow of SPIE.

Zetian Mi was recognized as a Most Highly Prolific Author in Nano Letters.

Protocol Activity Status:

Technology Transfer: Nothing to Report

Project Report

1. Statement of the Problem Studied

The transition-metal dichalcogenide (TMDC) semiconductors, including MoS_2, WS_2, $MoSe_2$, WSe_2, $MoTe_2$, and WTe_2 are indirect bandgap in their bulk case with a crossover to direct bandgap semiconductors in a monolayer limit due to quantum confinement effects [1, 2]. In the past few years, there has been a great deal of theoretical and experimental work to understand the evolution of optical properties and to analyze the electronic band structure of TMDCs [1-4]. Recent studies have further suggested that these two-dimensional (2D) materials are promising candidates for ultimate miniaturized, efficient nanophotonic devices including light emitting diodes (LEDs) [5], lasers [6, 7], solar cells [8], and photodetectors [9] due to their high optical absorption [5, 8], strong luminescence emission [9-12], large exciton binding energy [13] and relatively high carrier mobility [14, 15]. Significantly, the exciton oscillator strengths in such layer-structured 2D materials are exceptionally large, due to the very large exciton binding energies (0.5 – 1 eV). Therefore, such emerging 2D materials provide a nearly ideal platform for the exploitation of exciton-polaritons, the mixed states of photon and exciton, to realize room-temperature operational ultralow threshold polariton lasers with phase coherence and intensity stability comparable to that of conventional photon lasers.

To date, however, it has remained a grand challenge for the controlled synthesis of these novel 2D materials and related van der Waals heterostructures with supreme quality and clean interfaces. Hexagonal boron nitride (*h*-BN) is an ideal template for the growth of TMDCs, which can lead to reduced dielectric screening and large exciton binding energy. Moreover, in order to achieve efficient nanophotonic devices, the valence band maximum and conduction band minimum should both reside at the *K* point and be localized to the same monolayer, *i.e.*, *type-I* band alignment. Among the currently reported TDMC heterostructures, *h*-BN/TDMC/*h*-BN is the only one fulfilling the requirement. There is, therefore, an urgent need to develop growth/synthesis techniques for the monolithic integration of *h*-BN and TDMC. Molecular beam epitaxy (MBE), the champion semiconductor growth technology which offers ultimate control down to atomic layer in an ultrahigh vacuum environment, could potentially provide the solution. In this project, we have investigated the MBE growth and fundamental structural and optical properties of WTe_2 and WSe_2. ***The controlled synthesis of monolayer and multi-layer WTe_2 and WSe_2 has been successfully demonstrated by using MBE, which exhibit excellent structural and optical properties. We have further investigated the MBE growth of h-BN and demonstrated h-BN with excellent optical properties.*** At a relatively high growth temperature of 1100-1300 °C, it is observed that h-BN can exhibit strong excitonic emission at room-temperature, with defect-related emission largely suppressed. In this work, we have also demonstrated, for the first time, single crystalline 2D TMDCs grown directly on amorphous template. ***The capacity to epitaxially grow superior quality monolayer TMDC and h-BN by MBE provides a viable approach for the monolithic integration of various monolayer 2D heterostructures and nanostructures with access to unprecedented material quality, complexity, and degree of control, which is critical for their emerging device applications, including the realization of high temperature polariton lasers.***

2. Summary of the Most Important Results

2.1. Molecular beam epitaxy and characterization of WTe_2

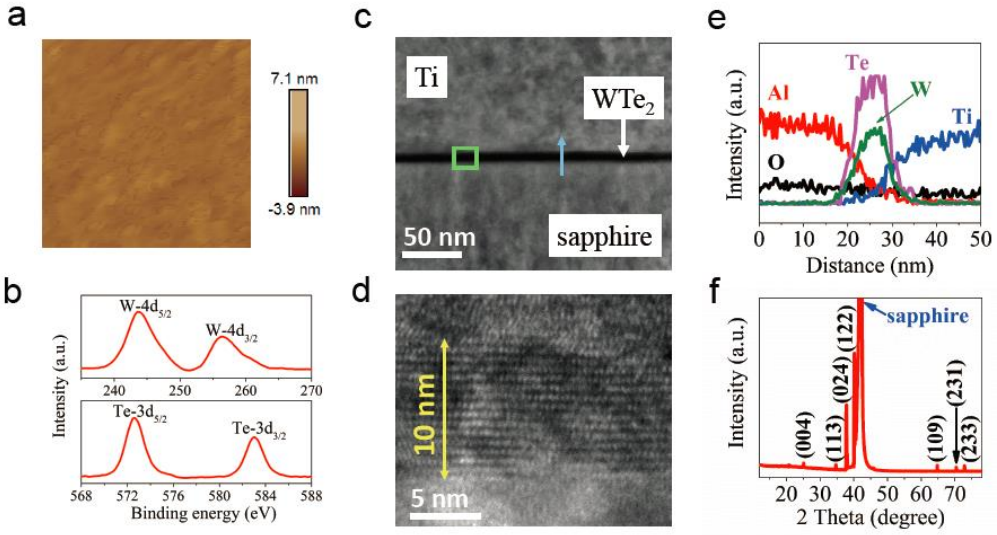

Figure 1 Surface, structure and electrical properties of MBE grown WTe_2 on sapphire. (a) The surface morphology measured by atomic force microscopy, showing smooth surface with a roughness of 0.22 nm. (b) High-resolution XPS core-level peaks of W (4d orbit) and Te (3d orbit). (c) Low-magnification side-view TEM image of WTe_2 on sapphire with titanium protection layer on top. The rectangular region bordered by green dashed lines is for high-resolution TEM analysis (Fig. 1d), and the EDX line scan analysis is performed along the blue arrow. (d) High-resolution cross-sectional TEM image shows clearly layered structure with an interplanar spacing of 0.667 nm. (e) High-resolution line-scan EDX profile, suggesting uniform distribution of W and Te. (f) X-ray diffraction in the Bragg-Brentano geometry with Miller indexes corresponding to Td-WTe_2 crystal structure.

We have first investigated the MBE growth of WTe_2. WTe_2 with a thickness of 10 nm was grown on c-Al_2O_3 (0001) substrate using a Veeco Genxplor MBE system. During the growth of WTe_2, the substrate temperature was 350 °C. A PBN effusion cell and an e-beam evaporator were used for the thermal evaporation of Te and W, respectively. The Te flux was measured to be 5×10^{-8} Torr. The growth rate was estimated to be 0.12 nm/min. The use of a very slow deposition rate is to reduce the formation of Te vacancies. Shown in Fig. 1(a) is the atomic force microscopy (AFM) image of the WTe_2 film, which exhibits smooth and continuous surface morphology. The surface roughness is estimated to be 0.22 nm, without the presence of any sharp edges, wrinkles, or discontinuity. The stoichiometric analysis was performed by high-resolution X-ray photoelectron spectroscopy immediately after growth. The core-level peaks of W (4d orbit) and Te (3d orbit) are shown in Fig. 1(b). The presence of W and Te oxidation peaks were not observed, confirming the high purity of epitaxial WTe_2. The atomic percentage ratio of W and Te was measured to be 1:1.93, suggesting the formation of nearly stoichiometric WTe_2. Structural properties of WTe_2 was studied using cross-sectional transmission electron microscopy (TEM). Shown in Fig. 1(c) is the low-magnification TEM image, confirming the formation of uniform and continuous film structure directly on sapphire substrate. Illustrated in

Fig. 1(d) is the high-resolution TEM image for the dashed green box in Fig. 1(c), which shows a distinct layered structure, with the atomic planes parallel to the sapphire/WTe_2 interface. The interplanar spacing along the growth direction is derived to be 0.667 nm, which is slightly smaller than that along the c-axis (0.7035 nm) of bulk WTe_2, suggesting the presence of tensile strain in the epitaxial WTe_2 on sapphire. The energy dispersive X-ray spectroscopy (EDX) scans were performed along the solid blue line in Fig. 1(c). The elemental distribution, including Al, O, W, Te and Ti (the top protection layer used in sample preparation) are shown in Fig. 1(e). It is seen that W and Te signals dominate for regions corresponding to the WTe_2 layer. The formation of an abrupt WTe_2/sapphire heterointerface is also evident based on the sharp increase of W and Te signals. Moreover, the W and Te signals remain relatively constant in the WTe_2 layer, suggesting uniform compositional distribution along the growth direction.

Structural characterization of WTe_2 films were further performed using X-ray diffraction. Shown in Fig. 1(f) is the theta-2theta scan. Multiple peaks corresponding to diffraction from the (024) and (122) planes can be clearly identified, which provides strong evidence that the epitaxial WTe_2 is of Td structure. In spite of the extremely thin layer, the linewidth is measured to be less than 0.2°, which demonstrates excellent crystallinity of MBE-grown WTe_2. Additionally, diffraction peaks corresponding to the (004), (113), (109), (231), and (233) planes were detected, which are consistent with theoretical and experimental studies of single crystal WTe_2 in the Td phase.

Detailed transport properties of epitaxial WTe_2 is being investigated. Preliminary results showed that the epitaxial WTe_2 were superconducting, with characteristic Kosterlitz-Thouless nonlinear voltage-current behavior, and an in-plane upper critical field more than seven times the Pauli paramagnetic limit. The result is consistent with large spin-orbit-coupling, and may indicate the unconventional nature of the superconducting ground state of the tilted Weyl electrons.

2.2. Molecular beam epitaxy and characterization of WSe_2

With the successful demonstration of MBE growth of WTe_2, we have further investigated the MBE growth and structural and optical characteristics of monolayer and multi-layer WSe_2. To demonstrate the van de Waals epitaxy of WSe_2, single crystalline monolayer, bilayer, and trilayer WSe_2 were grown directly on amorphous SiO_x template. The epitaxy was performed using a Veeco Genxplor MBE system. During the growth of WSe_2, the substrate temperature was kept at ~400 ºC. A PBN effusion cell and an e-bean evaporator were used for the thermal evaporation of Se and W sources, respectively. Se flux was measured to be ~3.5×10^{-7} Torr. The growth rate was estimated to be ~0.7 Å min^{-1}. After the growth is completed, the substrate temperature was increased to 650 °C for a 10 minute annealing under Se flux to further improve the material quality. During the epitaxy, reflection high-energy electron diffraction (RHEED) was used to monitor the growth process. RHEED is a widely used technique to distinguish the formation of single crystalline, polycrystalline, and amorphous structures during molecular beam epitaxy. Figure 2a shows the observation of streaky RHEED pattern during the epitaxy of monolayer WSe_2, suggesting the formation of single crystalline WSe_2. To our knowledge, this is the first demonstration of direct epitaxy of crystalline WSe_2 on amorphous substrate/template. Stoichiometric analysis was performed by high-resolution X-ray photoelectron spectroscopy

(XPS). Shown in Fig. 2b, the atomic percentage ratio of W and Se was measured to be ~1:2, suggesting the formation of stoichiometric WSe_2. Moreover, the absence of W and Se oxidation peaks confirms the high purity of epitaxial WSe_2. In addition, Figure 2c shows a typical optical microscopy image of WSe_2 monolayer with a thickness of ~0.8 nm measured by atomic force microscopy (AFM).

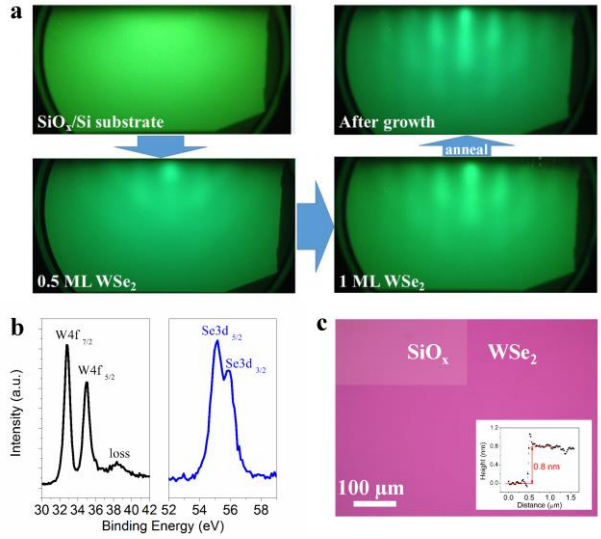

Figure 2 Growth and characterization of monolayer WSe_2 directly on SiO_x. (a) In-situ observations of RHEED patterns during MBE growth of WSe_2 monolayer on SiO_x/Si substrates. (b) XPS spectra of W and Se core-level peaks. The atomic percentage ratio of W and Se was determined to be ~1:2. (c) Optical microscopy image of bare SiO_x/Si substrate and as-grown WSe_2 monolayer sample. Part of the WSe_2 film was intentionally removed to expose SiO_x surface. The inset is an AFM height measurement revealing a thickness of ~0.8 nm corresponding to monolayer WSe_2.

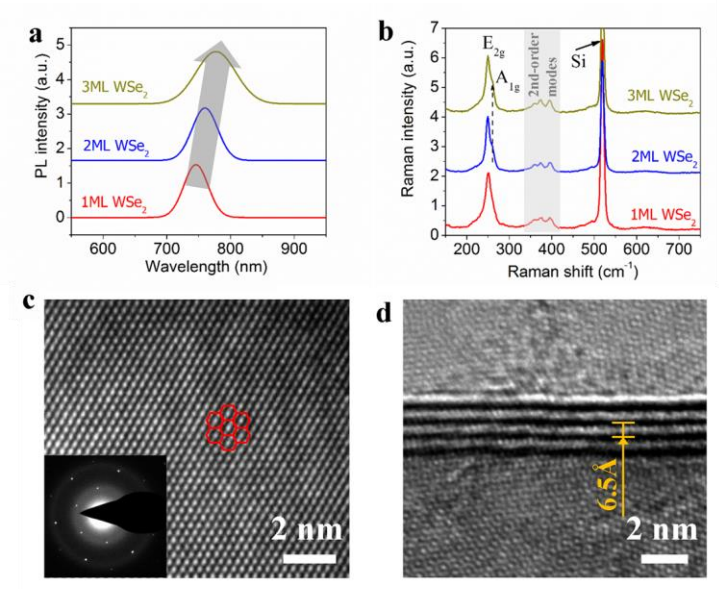

Figure 3 (a) Photoluminescence spectra of 1-3 ML WSe_2. The arrow indicates the reduced energy gap of WSe_2 with increasing thickness. (b) Micro-Raman spectra of 1-3 ML WSe_2 samples measured at room temperature. E_{2g} peak at ~250.8 cm^{-1} indicates WSe_2 crystals. (c) High-resolution plane-view TEM image of monolayer WSe_2. The inset corresponds to the selected area electron diffraction pattern. The solid hexagons represent W atomic distribution of 2H-WSe_2 crystal. (d) Side view of multilayer WSe_2 revealing the layer-by-layer stacking structure.

We have further studied the photoluminescence and Raman properties of 1-3 ML WSe_2. Figure 3a compares the photoluminescence spectra of 1-3 ML WSe_2 samples measured at room temperature. It is seen that, with increasing thickness, the energy gap shows a decreasing trend, which approaches to ~1.2 eV of bulk WSe_2. Thickness-dependent Raman scattering spectra measured at room temperature are shown in Fig. 3b. One in-plane vibration mode E_{2g} at ~250.8 cm^{-1} was observed, which confirms the formation of WSe_2. The shoulder peak A_{1g} at ~260.2 cm^{-1}, representing the out-of-plane vibration, is undetected in monolayer sample but is present in multi-layer structures. There are also several weak modes at 350~400 cm^{-1}, which represent the second-order vibration modes for WSe_2. Structural properties of epitaxial WSe_2 are further investigated using high-resolution transmission electron microscopy. The selected area electron diffraction (SAED) pattern within six fold symmetry, shown in Fig. 3c, demonstrates the crystal structure with a hexagonal lattice. Figure 3d reveals the formation of multi-layer WSe_2 film. The interlayer spacing is determined to be ~0.65 nm for one WSe2 layer, which is consistent with theoretical calculation and other reports.

2.3. Molecular beam epitaxy and characterization of hexagonal boron nitride

The controllable formation of heterostructures with superior interface properties is essentially required for practical electronic and photonic device applications. A range of TMDC heterostructures, including TMDC/BN, TMDC/graphene, and TMDC/TMDC have been demonstrated with the use of mechanical transfer process. It has remained difficult, however, to achieve TMDC heterostructures with pristine interface properties. Moreover, the heterostructure size is only limited to micrometer scale. In this regard, we have further investigated the MBE growth of BN, which can serve as a pristine template for the epitaxy of monolayer TMDCs and enable the monolithic integration TMDC/BN heterostructures.

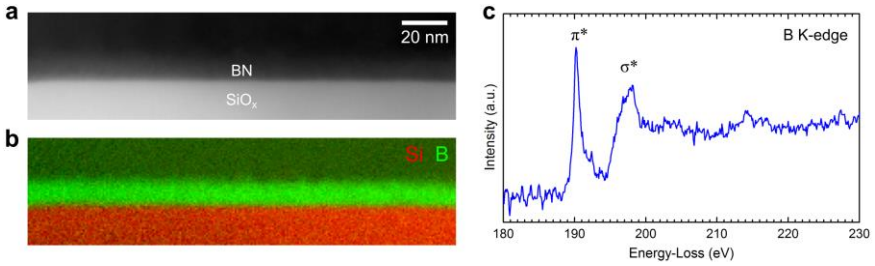

Figure 4 (a) STEM-HAADF image of the h-BN layer grown on a SiO_x/Si(001) substrate by molecular beam epitaxy. (b) EELS elemental mapping of the distribution of B and Si at the h-BN/SiO_x interface using the B K and Si $L_{2,3}$-edges, respectively. (c) Core-loss EELS spectra of the B K-edge from the BN layer showing both π* and σ* components, confirming hexagonal-BN.

To date, the achievement of high quality BN by direct epitaxial growth has remained challenging. By combining a unique e-beam source for boron evaporation with a nitrogen plasma-assisted MBE system, we have demonstrated the growth of hexagonal BN on a wide range of substrates, including sapphire, nickel, and Si. The growth of *h*-BN was conducted at substrate temperatures varying from 500 °C to 1300 °C, by evaporating boron with a relatively low rate (< 0.1 Å/s), measured with an Inficon Guardian EIES controller, a nitrogen flow rate of

0.3 to 2 sccm and RF plasma forward power of 350 W. Samples with *h*-BN thicknesses ranging from 1.5 nm to 10 nm were grown. Shown in Fig. 4a is the STEM-HAADF image of BN layer grown directly on SiO_x on Si(001) substrate. The EELS elemental mapping of the distribution of boron and silicon at the h-BN/SiO_x interface using the B K and Si $L_{2,3}$-edges is shown in Fig. 4b. Illustrated in Fig. 4c, the fine-structures of the B K-edge show the presence of peaks characteristic of $1s \rightarrow \pi^*$ (191.5 eV) and $1s \rightarrow \sigma^*$ (198.5 eV) transitions, which indicate sp^2-hybridization identifying the layers as hexagonal-BN.

We have also observed that the quality of *h*-BN depends critically on the substrate temperature. For growth temperature below 1000 °C, defect-related photoluminescence emission often dominates. By optimizing the growth temperature (> 1100 °C) and N flow rate, we have demonstrated superior *h*-BN, evidenced by the strong Raman and photoluminescence emission, shown Figs. 5a and b, respectively. The two emission peaks shown in Fig. 5b are attributed to the free exciton and bound exciton emission, respectively.

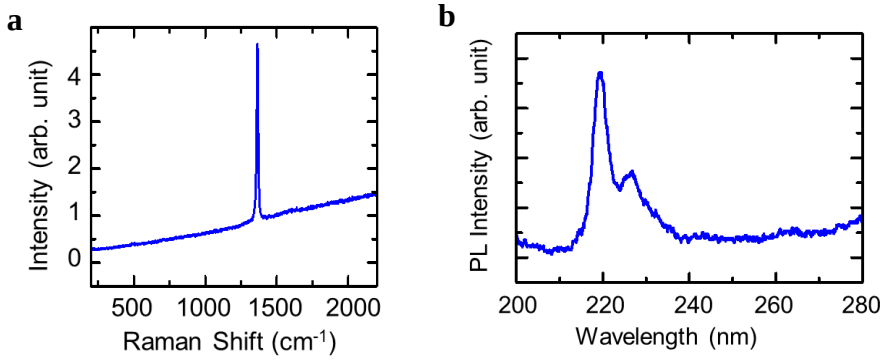

Figure 5 (a) Raman and (c) photoluminescence spectrum of *h*-BN grown by MBE.

3. Publications

1. "Effect of growth temperature on the structural and optical properties of hexagonal boron nitride by molecular beam epitaxy", D. A. Laleyan, S. Zhao, Y. Wang and Z. Mi, Appl. Phys. Lett., in preparation.
2. "Magnetic-field-enhanced superconductivity in epitaxial thin film WTe_2", T. Asaba, Y. Wang, G. Li, B. J. Lawson, C. Tinsman, L. Chen, S. Zhao, D. Laleyan, Z. Mi, L. Li, Phys. Rev. Lett., under review.
3. "Wafer-scale synthesis of monolayer WSe_2: A multi-functional photocatalyst for efficient overall pure water splitting", Y. Wang, S. Zhao, Y. Wang, D. Laleyan, C.-H. Soh, Y. Wu, and Z. Mi, Nano Lett., in preparation.

4. Report of Inventions

None.

5. List of Scientific Personnel Supported, Degrees, Awards and Honors

David Laleyan (PhD student)

Zetian Mi was elected Fellow of SPIE.

Zetian Mi was recognized as a Most Highly Prolific Author in Nano Letters.

6. Technology Transition

None.

Bibliography:

1. A. Splendiani, L. Sun, Y. Zhang, T. Li, J. Kim, C. Y. Chim, G. Galli, and F. Wang, "Emerging photoluminescence in monolayer MoS_2," *Nano Lett.*, **10** (4)**,** 1271-1275 (2010).
2. A. Kuc, N. Zibouche, and T. Heine, "Influence of quantum confinement on the electronic structure of the transition metal sulfide TS_2," *Phys. Rev. B*, **83** (24)**,** 245213 (2011).
3. K. F. Mak, C. Lee, J. Hone, J. Shan, and T. F. Heinz, "Atomically Thin MoS_2: A New Direct-Gap Semiconductor," *Phys. Rev. Lett.*, **105** (13)**,** 136805 (2010).
4. Z. Y. Zhu, Y. C. Cheng, and U. Schwingenschlögl, "Giant spin-orbit-induced spin splitting in two-dimensional transition-metal dichalcogenide semiconductors," *Phys. Rev. B*, **84** (15)**,** 153402 (2011).
5. J. S. Ross, P. Klement, A. M. Jones, N. J. Ghimire, J. Yan, D. G. Mandrus, T. Taniguchi, K. Watanabe, K. Kitamura, W. Yao, D. H. Cobden, and X. Xu, "Electrically tunable excitonic light-emitting diodes based on monolayer WSe_2 p-n junctions," *Nature Nanotech.*, **9** (4)**,** 268-272 (2014).
6. O. Salehzadeh, M. Djavid, N. H. Tran, I. Shih, and Z. Mi, "Optically Pumped Two-Dimensional MoS_2 Lasers Operating at Room-Temperature," *Nano Lett.*, **15** (8)**,** 5302-5306 (2015).
7. S. Wu, S. Buckley, J. R. Schaibley, L. Feng, J. Yan, D. G. Mandrus, F. Hatami, W. Yao, J. Vuckovic, A. Majumdar, and X. Xu, "Monolayer semiconductor nanocavity lasers with ultralow thresholds," *Nature*, **520** (7545)**,** 69-72 (2015).
8. M. Bernardi, M. Palummo, and J. C. Grossman, "Extraordinary Sunlight Absorption and One Nanometer Thick Photovoltaics Using Two-Dimensional Monolayer Materials," *Nano Lett.*, **13** (8)**,** 3664-3670 (2013).
9. O. Lopez-Sanchez, D. Lembke, M. Kayci, A. Radenovic, and A. Kis, "Ultrasensitive photodetectors based on monolayer MoS_2," *Nature Nanotech.*, **8** (7)**,** 497-501 (2013).
10. A. Hangleiter, "Recombination of correlated electron-hole pairs in two-dimensional semiconductors," *Phys. Rev. B*, **48** (12)**,** 9146-9149 (1993).
11. A. Kumar and P. K. Ahluwalia, "Mechanical strain dependent electronic and dielectric properties of two-dimensional honeycomb structures of MoX_2 (X=S, Se, Te)," *Physica B Condens. Matter*, **419** 66-75 (2013).
12. C. Ataca, M. Topsakal, E. AktüRk, and S. Ciraci, "A Comparative Study of Lattice Dynamics of Three- and Two-Dimensional MoS_2," *J. Phys. Chem. C*, **115** (33)**,** 16354-16361 (2011).
13. H. Peelaers and C. G. Van De Walle, "Effects of strain on band structure and effective masses in MoS_2," *Phys. Rev. B*, **86** (24)**,** 241401 (2012).
14. T. Korn, S. Heydrich, M. Hirmer, J. Schmutzler, and C. SchüLler, "Low-temperature photocarrier dynamics in monolayer MoS_2," *Appl. Phys. Lett.*, **99** (10)**,** 102109 (2011).
15. H. Y. Shi, R. S. Yan, S. Bertolazzi, J. Brivio, B. Gao, A. Kis, D. Jena, H. G. Xing, and L. B. Huang, "Exciton Dynamics in Suspended Mono layer and Few-Layer MoS_2 2D Crystals," *ACS Nano*, **7** (2)**,** 1072-1080 (2013).